Surgical and Radiologic Anatomy (2019) 41:985–1001
https://doi.org/10.1007/s00276-019-02256-1

ORIGINAL ARTICLE

Atlas posterior arch and vertebral artery's groove variants: a classification, morphometric study, clinical and surgical implications

Konstantinos Natsis[1] · Evangelia-Theophano Piperaki[2] · Moschos Fratzoglou[3] · Nikolaos Lazaridis[1] · Parmenion P. Tsitsopoulos[4] · Alexandros Samolis[5] · Michael Kostares[5] · Maria Piagkou[5]

Received: 10 November 2018 / Accepted: 9 May 2019 / Published online: 6 June 2019

Abstract

Background The third part of the vertebral artery (VA) coursing in vertebral artery groove (VAG) may be injured during posterior craniocervical junction approaches.

Objective The current study classifies all possible variants of the posterior arch (PA) of the atlas vertebra (C_1), focusing on VAG and calculates their incidence. PA and VAG morphometry is studied in correlation with gender and age. Clinical and surgical implications of recorded variants are provided in an effort to explain associated pathology. The usefulness of three-dimensional computed tomography (3D-CT) in detecting PA variants is highlighted.

Materials and methods Two hundred and forty-four Greek adult dry C_1 were classified in types according to PA morphology [i.e. presence of an imprint or a distinct VAG and occurrence of a partially or completely ossified dorsal (PDP or CDP) or lateral (PLP or CLP) ponticle unilaterally or bilaterally]. Combined variants were also included.

Results A VAG and an imprint were detected in 42.62% and 15.16%. A PDP and CDP were observed in 18.03% and 15.98%, while a CLP and PLP in 2.05% and 1.64%, respectively. Combined PDP and PLP were detected in 2.05%, a CDP and CLP similarly to a CDP and PLP in 1.23% and a PDP and CLP in 0.40%.

Conclusions Variants' classification will contribute to an in depth understanding of the complex C_1 anatomy and may explain cases of VA entrapment and injury during PA fixation. Surgeons should carefully study 3D-CT imaging to ensure type, location, size and shape of C_1 ponticles in combination with VAG morphology and VA course before screw insertion.

Keywords Atlas vertebra · Posterior arch · Posterior ponticle · Lateral ponticle · Vertebral artery groove · Variation · Ossification

Konstantinos Natsis and Maria Piagkou equally contributed to the paper.

✉ Konstantinos Natsis
natsis@auth.gr

[1] Department of Anatomy and Surgical Anatomy, Faculty of Health Sciences, School of Medicine, Aristotle University of Thessaloniki, Thessaloniki, Greece

[2] Department of Microbiology, School of Medicine, National and Kapodistrian University of Athens, Athens, Greece

[3] Department of Neurosurgery, General District Hospital of Nikaia, Piraeus, Greece

[4] Department of Neurosurgery, Hippokratio General Hospital, School of Medicine, Aristotle University of Thessaloniki, Thessaloniki, Greece

[5] Department of Anatomy, Faculty of Health Sciences, School of Medicine, National and Kapodistrian University of Athens, Athens, Greece

Abbreviations

C1	Atlas vertebra
PA	Posterior arch
VA	Vertebral artery
VAG	Vertebral artery groove
I	Imprint
DP	Dorsal ponticle
LP	Lateral ponticle
PDP	Partially ossified dorsal ponticle
CDP	Completely ossified dorsal ponticle
PLP	Partially ossified lateral ponticle
CLP	Completely ossified lateral ponticle
DLP	Dorsolateral ponticle
LM	Lateral mass
TP	Transverse process
TF	Transverse foramen
AF	Arcuate foramen
RTF	Retrotransverse foramen

R	Right side
L	Left side
D1	Linear distance of vertebral artery groove from the posterior midline to the most medial edge of vertebral artery groove on the inner cortex
D2	Linear distance of vertebral artery groove from the posterior midline to the most medial edge of vertebral artery groove on the outer cortex
D3	Linear distances of vertebral artery groove from the posterior midline to the most lateral edge of vertebral artery groove to the inner cortex
D4	Linear distances of vertebral artery groove from the posterior midline to the most lateral edge of vertebral artery groove to the outer cortex
TEM	Technical error of measurement
rTEM	Relative technical error of measurement
R	Coefficient of reliability

Introduction

The first cervical vertebra (C_1) has an atypical ring-like form with an anterior arch, a posterior arch (PA) and two lateral masses (LM). Its two transverse processes (TP) are perforated by the transverse foramina (TF) transmitting the vertebral arteries (VA), vertebral veins and sympathetic plexus. Dorsal and lateral ponticles (DP and LP) (complete or partial) are occasionally observed [23].

The DP is formed due to a complete ossification extending from the dorsal edge of C_1 superior facet to the distal portion of vertebral artery groove (VAG). The osseous bridge is also characterized as posterior oblique and the ensuing foramen, as retroarticular or arcuate foramen (AF) [22, 25]. The LP created after the complete ossification from the lateral edge of C_1 superior facet over VAG to the TP is also named as lateral [22, 25] or lateroglenoidal bridge [30], and the created foramen is characterized as supratransverse foramen [5]. In cases of DP and LP coexistence, the so-called dorsolateral ponticle (DLP), the foramen located at the upper portion of DLP, serves as a passage of the greater occipital nerve and a small vein. C_1 ponticles are often a legacy or an adaptive evolution within the same species [23].

Knowledge of C_1 variable anatomy is fundamental in spine surgery (*decompression, plate osteosynthesis, posterior cervical arthrodesis, wiring, LM and pedicle screw fixation*) requiring PA exposure. Below and lateral to the VAG, the thinnest part of PA, found posteriorly to the LM, is a typical anatomical point for screw placement [4]. VAG varies in form ranging from an impression to a groove or a sulcus. Variable morphology is of paramount importance, since the third part of VA situated in VAG may be injured during posterior craniovertebral approaches, causing serious complications [43]. Thus, the VAG pre-operative imaging is essential to identify the exact position of VA, enhancing surgical safety.

The current study classifies any possible morphological PA variant focusing on VAG and records its incidence, since according to Hasan et al. classification [16] lack of transition types does not allow comparisons and safe conclusions. In addition, VAG and PA morphometry are studied in correlation with gender and age. Clinical and surgical implications of VAG variants and PA morphometric details are also provided in an effort to explain associated pathology and safety of surgical manipulations. The usefulness and importance of three-dimensional computed tomography (3D-CT) in PA variant evaluation, as well as the 3D-CT angiography (3D-CTA) for the variable course of VA and risk of injury is highlighted.

Materials and methods

Three hundred dry C_1 of a Greek population from the osseous collection of the Department of Anatomy and Surgical Anatomy of the Aristotle University of Thessaloniki were investigated. Vertebrae of children, damaged and pathological vertebrae were excluded, as well as vertebrae of unknown gender and age, and cases of PA hypoplasia or clefts, and other ossifications in the TP area, i.e. the epitransverse process variant were analyzed. Thus, 244 (125 male and 119 female) adult dry C_1 of Greek population were included and subdivided in three age groups: 20–39 years (52 C_1), 40–59 years (70 C_1), 60 and above (122 C_1) to examine age effect in C_1 morphometry. All vertebrae were derived from body donors' cadavers (donation before death after written informed consent). Thus, evidence concerning age of death and gender, and cause of death was known.

Each C_1 was categorized according to identification of morphology of the left side (L), right side (R) and both sides at the PA focusing on VAG. The ossification extent (partial or/and complete) was taken into consideration. On VAG area, the presence of an imprint or a groove was considered as a typical form. Sulcus is characterized by a very deep groove. Following a meticulous observation, C_1 were classified in types according to the presence of an imprint at PA, the existence of a distinct VAG and the occurrence of PDP, CDP, PLP and CLP. Isolated and combined morphological variants were classified into types (Table 1).

Type 1 Imprint (I) at PA was assigned as number 1. Adding L and R, the subtypes 1L and 1R or IL and IR will ensue.

Type 2 Distinct VAG with number 2. Adding L and R, the subtypes 2L and 2R or VAGL and VAGR will ensue.

Type 3 Partial DP (PDP) with number 3. Adding L and R, the subtypes 3L and 3R or PDPL and PDPR will ensue.

Type 4 Complete DP (CDP) with number 4. Adding L and R, the subtypes 4L and 4R or CDPL and CDPR will ensue.

Table 1 Methodology of classification of all types of anatomical variants of C_1 according to the presence of dorsal and/or lateral ponticles (DP and/or LP)

TYPE 1=I (Imprint at L and R and all possible combinations)					
Subtypes	**Number**	**Abbreviations**	**N/Incidence (%)**	**C_1 schematic representation**	**Dry C_1 figure**
1.1	**1L-1R**	**IL-IR**	**8 (3.27%)**		
1.2	**1L-2R**	**IL -VAGR**	**21 (8.60%)**		
1.3	**1L-3R**	**IL- PDPR**	**5 (2.05%)**	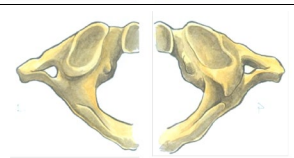	
1.4	**1L-4R**	**IL-CDPR**	**3 (1.23%)**		
1.5	1L-5R	IL-PLPR	Not found		
1.6	1L-6R	IL- CLPR	Not found		
1.7	1L-7R	IL-(PPP and PLP)R	Not found		
1.8	1L-8R	IL-(CDP and CLP)R	Not found		
1.9	1L-9R	IL-(PDP and CLP)R	Not found		
1.10	1L-10R	IL-(CDP and PLP)R	Not found		
Total cases 37 (15.16%)					
TYPE 2= VAG (Vertebral artery groove at L and R and all possible combinations)					
Subtypes	**Number**	**Abbreviations**	**N/Incidence (%)**	**C_1 schematic representation**	**Dry C_1 figure**
2.2	**2L-2R**	**VAGL-VAGR**	**85 (34.83%)**		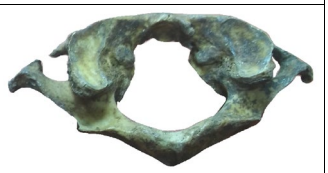
2.1	**2L-1R**	**VAGL -IR**	**3 (1.23%)**		
2.3	**2L-3R**	**VAGL- PDPR**	**12 (4.91%)**		
2.4	**2L-4R**	**VAGL-CDPR**	**3 (1.23%)**		

Table 1 (continued)

					
2.5	**2L-5R**	**VAGL-PLPR**	**1 (0.40%)**		
2.6	2L-6R	VAGL- CLPR	Not found		
2.7	2L-7R	VAGL-(PPP and PLP)R	Not found		
2.8	2L-8R	VAGL-(CDP and CLP)R	Not found		
2.9	2L-9R	VAGL-(PDP and CLP)R	Not found		
2.10	2L-10R	VAGL-(CDP and PLP)R	Not found		
Total cases 104 (42.62%)					
TYPE 3= PDP (Partial dorsal ponticle at L and R and all possible combinations)					
Subtypes	**Number**	**Abbreviations**	**N/Incidence (%)**	**C_1 schematic representation**	**Dry C_1 figure**
3.3	**3L-3R**	**PDPL- PDPR**	**19 (7.78%)**		
3.1	**3L-1R**	**PDPL-IR**	**3 (1.23%)**	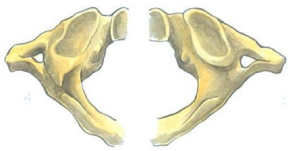	
3.2	**3L-2R**	**PDPL-VAGR**	**13 (5.32%)**		
3.4	**3L-4R**	**PDPL-CDPR**	**8 (3.27%)**		
3.5	**3L-5R**	**PDPL-PLPR**	**1 (0.40%)**		
3.6	3L-6R	PDPL- CLPR	Not found		
3.7	3L-7R	PPPL-(PPP and PLP)R	Not found		
3.8	3L-8R	PDPL-(CDP and CLP)R	Not found		
3.9	3L-9R	PDPL-(PDP and CLP)R	Not found		
3.10	3L-10R	PDPL-(CDP and PLP)R	Not found		
Total cases 44 (18.03%)					
TYPE 4 = CDP (Complete dorsal ponticle at L and R and all possible combinations)					
Subtypes	**Number**	**Abbreviations**	**N/Incidence (%)**	**C_1 schematic representation**	**Dry C_1 figure**

Table 1 (continued)

4.4	**4L-4R**	**CDPL-CDPR**	**14 (5.73%)**	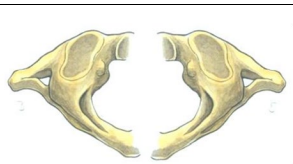	
4.1	**4L-1R**	**CDPL-IR**	**1 (0.40%)**		
4.2	**4L-2R**	**CDPL-VAGR**	**5 (2.04%)**		
4.3	**4L-3R**	**CDPL-PDPR**	**16 (6.55%)**		
4.5	**4L-5R**	**CDPL-PLPR**	**1 (0.40%)**		
4.6	4L-6R	CDPL- CLPR	Not found		
4.7	4L-7R	CDPL-(PDP and PLP)R	Not found		
4.8	**4L-8R**	**CDPL-(CDP and CLP)R**	**1(0.40%)**	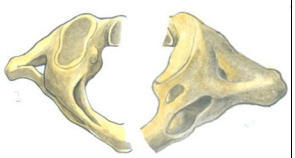	
4.9	4L-9R	CDPL-(PDP and CLP)R	Not found		
4.10	**4L-10R**	**CDPL-(CDP and PLP)R**	**1 (0.40%)**		
Total cases 39 (15.98%)					
TYPE 5 = PLP (Partial lateral ponticle at L and R and all possible combinations)					

Table 1 (continued)

Subtypes	Number	Abbreviations	N/Incidence (%)	C_1 schematic representation	Dry C_1 figure
5.5	**5L-5R**	**PLPL-PLPR**	**1 (0.40%)**		
5.1	5L-1R	PLPL-IR	Not found		
5.2	**5L-2R**	**PLPL-VAGR**	**1 (0.40%)**		
5.3	**5L-3R**	**PLPL-PDPR**	**1 (0.40%)**		
5.4	5L-4R	PLPL-CDPR	Not found		
5.6	5L-6R	PLPL- CLPR	Not found		
5.7	5L-7R	PLPL-(PPP and PLP)R	Not found		
5.8	5L-8R	PLPL-(CPP and CLP)R	Not found		
5.9	**5L-9R**	**PLPL-(PDP and CLP)R**	**1 (0.40%)**	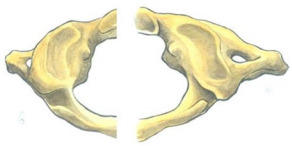	
5.10	5L-10R	PLPL-(CPP and PLP)R	Not found		
Total cases 4 (1.63%)					
TYPE 6 = CLP (Complete lateral ponticle at L and R and all possible combinations)					
Subtypes	**Number**	**Abbreviations**	**N/Incidence (%)**	**C_1 schematic representation**	**Dry C_1 figure**
6.6	**6L-6R**	**CLPL-CLPR**	**1 (0.40%)**		
6.1	**6L-1R**	**CLPL-IR**	**1 (0.40%)**		
6.2	**6L-2R**	**CLPL-VAGR**	**1 (0.40%)**		
6.3	**6L-3R**	**CLPL-PDPR**	**1 (0.40%)**		
6.4	6L-4R	CLPL-CPPR	Not found		
6.5	6L-5R	CLPL- PLPR	Not found		

Table 1 (continued)

6.7	**6L-7R**	**CLPL-(PDP and PLP)R**	**1 (0.40%)**		
6.8	6L-8R	CLPL-(CDP and CLP)R	Not found		
6.9	6L-9R	CLPL-(PDP and CLP)R	Not found		
6.10	6L-10R	CLPL-(CDP and PLP)R	Not found		
Total cases 5 (2.04%)					
TYPE 7=PDP and PLP (Partial dorsolateral ponticle at L and R and all possible combinations)					
Subtypes	**Number**	**Abbreviations**	**N/Incidence (%)**	**C_1 schematic representation**	**Dry C_1 figure**
7.7	7L-7R	(PDP and PLP)L-(PDP and PLP)R	Not found		
7.1	7L-1R	(PDP and PLP)L-IR	Not found		
7.2	7L-2R	(PDP and PLP)L-VAGR	Not found		
7.3	**7L-3R**	**(PDP and PLP)L-PDPR**	**3 (1.23%)**		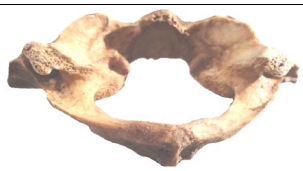
7.4	7L-4R	(PDP and PLP)L-CDPR	Not found		
7.5	7L-5R	(PDP and PLP)L- PLPR	Not found		
7.6	7L-6R	(PDP and PLP)L- CLPR	Not found		
7.8	**7L-8R**	**(PDP and PLP)L-(CDP and CLP)R**	**1 (0.40%)**		
7.9	7L-9R	(PDP and PLP)L-(PDP and CLP)R	Not found		
7.10	**7L-10R**	**(PDP and PLP)L-(CDP and PLP)R**	**1 (0.40%)**		
Total cases 5 (2.04%)					
TYPE 8=CDP and CLP (Complete dorsolateral ponticle at L and R and all possible combinations)					
Subtypes	**Number**	**Abbreviations**	**N/Incidence (%)**	**C_1 schematic representation**	**Dry C_1 figure**
8.8	8L-8R	(CDP and CLP)L-(CDP and CLP)R	Not found		
8.1	8L-1R	(CDP and CLP)L-IR	Not found		
8.2	8L-2R	(CDP and CLP)L –VAGR	Not found		
8.3	**8L-3R**	**(CDP and CLP)L –PDPR**	**1 (0.40%)**		
8.4	**8L-4R**	**(CDP and CLP)L –CDPR**	**1 (0.40%)**		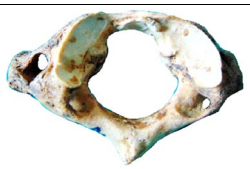
8.5	8L-5R	(CDP and CLP)L – PLPR	Not found		
8.6	8L-6R	(CDP and CLP)L – CLPR	Not found		
8.7	8L-7R	(CDP and CLP)L-(PDP and PLP)R	Not found		
8.9	8L-9R	(CDP and CLP)L-(PDP and CLP)R	Not found		

Table 1 (continued)

8.10	**8L-10R**	**(CDP and CLP)L-(CDP and PLP)R**	**1 (0.40%)**	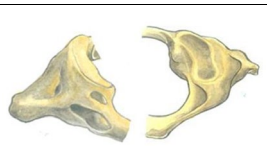	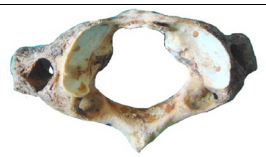
Total cases 3 (1.23%)					
TYPE 9=PDP and CLP (Partial dorsal and complete lateral ponticle at L and R and all possible combinations)					
Subtypes	**Number**	**Abbreviations**	**N/Incidence (%)**	**C_1 schematic representation**	**Dry C_1 figure**
9.9	9L-9R	(PDP and CLP)L-(PDP and CLP)R	Not found		
9.1	9L-1R	(PDP and CLP)L-IR	Not found		
9.2	9L-2R	(PDP and CLP)L –VAGR	Not found		
9.3	9L-3R	(PDP and CLP)L –PDPR	Not found		
9.4	9L-4R	(PDP and CLP)L –CDPR	Not found		
9.5	**9L-5R**	**(PDP and CLP)L – PLPR**	**1 (0.40%)**		
9.6	9L-6R	(PDP and CLP)L – CLPR	Not found		
9.7	9L-7R	(PDP and CLP)L-(PDP and PLP)R	Not found		
9.8	9L-8R	(PDP and CLP)L-(CDP and CLP)R	Not found		
9.10	9L-10R	(PDP and CLP)L-(CDP and PLP)R	Not found		
Total cases 1 (0.40%)					
TYPE 10=CDP and PLP (Complete dorsal and partial lateral ponticle at L and R and all possible combinations)					
Subtypes	**Number**	**Abbreviations**	**N/Incidence (%)**	**C_1 schematic representation**	**Dry C_1 figure**
10.10	**10L-10R**	**(CDP and PLP)L-(CDP and PLP)R**	**1(0.40%)**		
10.1	10L-1R	(CDP and PLP)L-IR	Not found		
10.2	**10L-2R**	**(CDP and PLP)L-VAGR**	**1(0.40%)**		
10.3	**10L-3R**	**(CDP and PLP)L-PDPR**	**1(0.40%)**		
10.4	10L-4R	(CDP and PLP)L-CDPR	Not found		
10.5	10L-5R	(CDP and PLP)L- PLPR	Not found		
10.6	10L-6R	(CDP and PLP)L- CLPR	Not found		
10.7	10L-7R	(CDP and PLP)L-(PDP and PLP)R	Not found		
10.8	10L-8R	(CDP and PLP)L-(CDP and CLP)R	Not found		
10.9	10L-9R	(CDP and PLP)L-(PDP and CLP)R	Not found		
Total cases 3 (1.23%)					

129 cases presented side symmetry (52.9%)

L left side, *R* right side, *DP* dorsal ponticle, *LP* lateral ponticle, *DLP* dorsolateral ponticle, *I* imprint, *VAG* vertebral artery groove, *PDP* partial dorsal ponticle, *CDP* complete dorsal ponticle, *PLP* partial lateral ponticle, *CLP* complete lateral ponticle, *PDP and PLP* combination of partial dorsal and partial lateral ponticle, *CDP and CLP* combination of complete dorsal and complete lateral ponticle, *PDP and CLP* combination of partial dorsal and complete lateral ponticle, *CDP and PLP* combination of complete dorsal and partial lateral ponticle

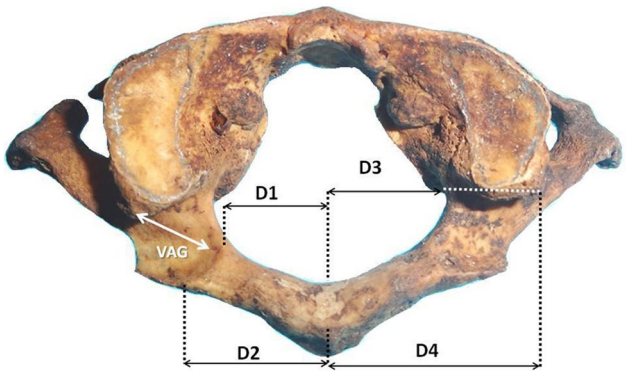

Fig. 1 Distances of vertebral artery groove (VAG) on the atlas superior surface from the posterior midline to the most medial edge of VAG on inner (D1) and outer (D2) cortices, and to the most lateral edge of VAG to the inner (D3) and outer (D4) cortices and black double arrows depict the distances

Fig. 2 The mean height of the posterior arch at the vertebral artery groove (VAG) or VAG thickness (yellow dotted line) and the minimum height of posterior arch at the outer part of VAG, proximal to the midline (white dotted line) (color figure online)

Type 5 Partial LP (PLP) with number 5. Adding L and R, the subtypes 5L and 5R or PLPL and PLPR will ensue.

Type 6 Complete LP (CLP) with number 6. Adding L and R, the subtypes 6L and 6R or CLPL and CLPR will ensue.

Type 7 Combination of PDP and PLP with number 7. Adding L and R, the subtypes 7L and 7R or (PDP and PLP) L and (PDP and PLP)R will ensue or PDLPL and PDLPR.

Type 8 Combination of CDP and CLP with number 8. Adding L and R, the subtypes 8L and 8R or (CDP and CLP) L and (CDP and CLP)R will ensue or CDLPL and CDLPR.

Type 9 Combination of PDP and CLP with number 9. Adding L and R, the subtypes 9L and 9R or (PDP and CLP) L and (PDP and CLP)R will ensue.

Type 10 Combination of CDP and PLP with number 10. Adding L and R, the subtypes 10L and 10R or (CDP and PLP)L and (CDP and PLP)R will ensue.

In cases of CDP, the AF length and width were measured. TF integrity and the retrotransverse foramen (RTF) presence (closed or dehiscent) were also recorded according to the side of occurrence. Minimum and maximum TF diameters were calculated.

The linear VAG distances on the superior surface of C_1 from the posterior midline to the most medial edge of VAG on inner (D1) and outer (D2) cortices were measured. Additionally, the linear distances of VAG from the posterior midline to the most lateral edge of VAG to the inner (D3) and outer (D4) cortices were calculated (Fig. 1a). VAG length on both sides was measured represented by the line connecting the midpoints of the medial and lateral ends of VAG (Fig. 1). The thickness of the lateral part of PA at VAG was also measured, as well as the PA length and minimum height (Fig. 2).

Measurements were taken with a Mitutoyo ABSOLUTE 500-196-20 Digital Caliper (0.001 mm accuracy). All measurements were repeated and technical error of measurement (TEM), relative technical error of measurement (rTEM) and coefficient of reliability (R) were calculated (Table 2). Descriptive statistics were evaluated for C_1 morphometric measurements and their statistical distribution was analyzed. Data normality was evaluated with the use of the Kolmogorov–Smirnov test, Wilcoxon signed ranks test was applied to investigate side asymmetry, Mann–Whitney *U* test and *t* test for gender dimorphism, and Kruskal–Wallis and one-way ANOVA tests to evaluate correlation with age. For all analyses, p value < 0.05 was considered statistically significant. Statistical analysis was carried out using IBM SPSS Statistics for Windows, version 21.0. The current study was a retrospective study and formal consent was not required.

Results

Variability in C1 ponticle classification

Type 2 was detected in 104 C_1 (42.62%), type 3 in 44 C_1 (18.03%), type 4 in 39 C_1 (15.98%), type 1 in 37 C_1 (15.16%), types 6 and 7 in 5 C_1 (2.05%), type 5 in 4 C_1 (1.64%), types 8 and 10 in 3 C_1 (1.23%) and type 9 in 1 C_1 (0.40%). CDP were observed in 54 C_1 (22.13%), 40 unilaterally [16.39%, 25L (10.24%) and 15R (6.15%)] and 14B (5.73%). CLP were observed in five C_1 (2.05%), four on the L side (1.64%) and 1B (0.41%). CDLP and PDLP were observed in 9 C_1 (3.69%) (6L, 2R and 1B) and 6 C_1 (2.46%) (5L and 1R). Mixed ossification DLP were observed in 8 C_1 (3.28%) (3L, 4R and 1B). Side symmetry existed in 129 C_1 (52.87%) (Table 1). DP (54.5%) were more commonly observed than LP (5.33%). 103 DP (62 males and 71 females) and 13 LP (5 males and 8 females) were detected. Both of them were ossified more commonly partially and unilaterally. Combined variants were detected in 23 C_1 (9.43%) (8 males and 15 females) (Table 3). A slight female preponderance is highlighted concerning the ossification extent in Greek C_1.

Table 2 Measurements by side

Measurement	TEM		rTEM %		*R*	
Side	Right	Left	Right	Left	Right	Left
TF max diameter	0.14	0.06	1.78	0.77	0.978	0.997
TF min diameter	0.06	0.10	1.05	1.57	0.993	0.990
VAG length	0.11	0.10	0.59	0.49	0.999	0.998
PA min height	0.08	0.05	1.91	1.26	0.995	0.997
PA height (outer of VAG)	0.07	0.05	0.83	0.62	0.998	0.999
D1	0.16	0.12	1.15	0.85	0.992	0.996
D2	0.18	0.25	1.03	1.34	0.993	0.989
D3	0.14	0.16	0.64	0.74	0.998	0.995
D4	0.22	0.18	0.85	0.67	0.989	0.996

TF transverse foramen, *VAG* vertebral artery groove, *PA* posterior arch, linear distance of VAG from the posterior midline to the most medial edge of VAG on inner (D_1) and outer (D_2) cortices and to the most lateral edge of VAG to the inner (D_3) and outer (D_4) cortices, *TEM* measure technical error, *rTem* relative technical error of measurement, *R* coefficient of reliability, *min* minimum and *max* maximum

Table 3 The occurrence of the variant features of C_1 in vertebral artery groove area of the posterior arch

Variant occurrence	*I*	VAG	PDP	CDP	PLP	CLP	PDP and PLP	CDP and CLP	PDP and CLP	CDP and PLP
Left side	29	19	25	25	3	4	5	6	1	2
Right side	8	42	35	15	4	0	1	2	1	3
Bilaterally	8	84	19	14	1	1	0	1	0	1
Total	45	145	79	54	8	5	6	9	2	6
%	18.44%	59.4%	32.37%	22.13%	3.27%	2.05%	2.45%	3.68%	0.81%	2.46%

I imprint, *VAG* vertebral artery groove, *PDP* partial dorsal ponticle, *CDP* complete dorsal ponticle, *PLP* partial lateral ponticle, *CLP* complete lateral ponticle

Transverse and Retrotransverse foramina (TF and RTF) morphology and morphometry

Four hundred and eighty-six TF were detected. TF were absent in two cases (0.41%) on the R, seven foramina (1.44%) were dehiscent on the R and three (0.62%) on the L. A single C_1 had bilaterally dehiscent TF and another C_1 had a TF in contact on the R. Complete TF were found in 475 cases (97.9%) [235 on the R (97.12%) and 241 on the L (98.8%)]. The mean TF max diameters on the R and L were: 7.86 ± 0.95 mm and 7.76 ± 1.07 mm and no gender dimorphism was observed (Table 4). Age had no significant impact (Table 5). The mean TF minimum diameters at the R and L were: 6.17 ± 0.77 mm and 6.17 ± 0.95 mm, and gender dimorphism existed (R—6.37 ± 0.72 mm in males and 5.97 ± 0.78 mm in females and L—6.34 ± 1.02 mm in males and 5.99 ± 0.83 mm in females) (Table 4). The age had no significant impact (Table 5). Side symmetry was observed for both diameters (Table 4).

A RTF was detected in 116 cases (complete in 41 cases on the R and in 27 cases on the L, and dehiscent in 22 cases on the R and in 26 cases on the L) (Figs. 3a, b and 4). The mean AF length and width was 6.70 ± 1.42 and 6.34 ± 1.35 mm on the R and 6.9 ± 0.3 mm and 6.6 ± 0.6 mm on the L, and side symmetry was detected ($p = 0.643$ and 0.551, paired-sample *T* test).

Posterior arch (PA) morphometry

The mean PA length was 50.65 ± 4.71 mm and gender dimorphism existed (higher mean values in males 52.2 ± 4.97 mm than females 48.97 ± 3.77 mm, $p = 0.003$). The mean PA height at the outer part of VAG, proximal to the midline was 8.32 ± 1.40 mm on the R and 8.21 ± 1.50 mm on the L. Side asymmetry and gender dimorphism existed on the R (8.61 ± 1.44 mm in males and 8.02 ± 1.29 mm in females) and L (8.43 ± 1.47 mm in males and 7.98 ± 1.49 mm in females) (Table 4). An increase in PA height was observed between first and second, and particularly between first and third age groups (Table 5).

The mean PA height at VAG (VAG thickness) was 4.13 ± 1.12 mm on the R and 3.86 ± 0.88 mm on the L, and asymmetry was found (Table 3). The mean VAG length was 18.9 ± 3.03 mm on the R and 19.97 ± 2.38 mm on the L, and asymmetry existed ($p = <0.001$), but no gender and age influence (Table 4). Only the age influenced the VAG

Table 4 Measurements by gender (125 male and 119 female vertebrae) and overall vertebrae (244 in number)

Total	Gender				Overall		*p** (to gender)	
	Male vertebrae		Female vertebrae					
	Mean ± SD		Mean ± SD		Mean ± SD			
Side	Right	Left	Right	Left	Right	Left	Right	Left
TF max diameter	7.98 ± 0.91	7.90 ± 1.19	7.73 ± 0.97	7.61 ± 0.91	7.86 ± 0.95	7.76 ± 1.07	0.113	0.117
**p* (to side)					*p* = 0.246			
TF min diameter	6.37 ± 0.72	6.34 ± 1.02	5.97 ± 0.78	6.00 ± 0.84	6.17 ± 0.77	6.17 ± 0.95	**0.002**	**0.034**
**p* (to side)					*p* = 0.914			
VAG length	19.19 ± 3.34	19.95 ± 2.71	18.60 ± 2.63	19.99 ± 1.97	18.90 ± 3.03	19.97 ± 2.38	0.248	0.920
**p* (to side)					*p* = <0.001			
PA height (outer of VAG)	8.61 ± 1.44	8.45 ± 1.47	8.02 ± 1.29	7.95 ± 1.49	8.32 ± 1.40	8.21 ± 1.50	**0.013**	**0.045**
**p* (to side)					*p* = <0.001			
PA min height	4.25 ± 1.09	4.11 ± 0.72	4.00 ± 1.14	3.60 ± 0.96	4.13 ± 1.12	3.86 ± 0.88	0.179	**< 0.001**
**p* (to side)					*p* = <0.001			
D1	13.91 ± 1.67	13.99 ± 1.76	13.50 ± 1.85	13.74 ± 1.80	13.71 ± 1.76	13.87 ± 1.78	0.237	0.466
**p* (to side)					*p* = 0.435			
D2	17.34 ± 2.02	18.69 ± 2.45	16.97 ± 2.28	18.23 ± 2.35	17.16 ± 2.15	18.46 ± 2.40	0.379	0.336
**p* (to side)					*p* = <0.001			
D3	21.18 ± 3.33	21.49 ± 1.77	21.57 ± 2.34	20.72 ± 2.52	21.37 ± 2.88	21.11 ± 2.20	0.495	0.076
**p* (to side)					*p* = 0.387			
D4	26.70 ± 2.03	27.39 ± 2.73	26.08 ± 2.19	26.95 ± 2.83	26.39 ± 2.12	27.17 ± 2.78	0.137	0.421
**p* (to side)					*p* = 0.003			

Bold values indicate the male predominance

**P* values from two-independent sample *t* tests

***P* values from paired-sample *t* tests

TF transverse foramen, *AF* arcuate foramen, *VAG* vertebral artery groove, *PA* posterior arch, linear distance of VAG from the posterior midline to the most medial edge of VAG on inner (D_1) and outer (D_2) cortices and to the most lateral edge of VAG to the inner (D_3) and outer (D_4) cortices

length on the L (Table 5). The distance from the midline to the most medial point of VAG on the inner cortex (D1) was 13.71 ± 1.76 mm on the R and 13.87 ± 1.78 mm on the L, and the outer cortex (D2) was 17.16 ± 2.15 mm on the R and 18.46 ± 2.40 mm on the L. The distance between the midline to the most lateral point of VAG on the inner cortex (D3) was 21.37 ± 2.88 mm on the R and 21.11 ± 2.20 mm on the L, and on the outer cortex (D4) was 26.39 ± 2.12 mm on the R and 27.17 ± 2.78 mm on the L. Side asymmetry was detected regarding the distances D2 and D4 (Table 4), and age influence concerning the distances D1, D2R, and D4 (Table 5).

Discussion

C_1 ponticles present a tendency towards reduction from lower to higher primates with the lowest frequencies observed in humans [23]. In humans, the head's load is received by C_1 superior facets; thus the ossified bridge disappears, as a result of natural selection or orthogenesis [34]. Although a number of theories concerning DP formation have been proposed, a clear explanation still remains a matter of debate. Some investigators supported that the DP is formed due to the superior oblique ligament's persistence [25], while others [42] mentioned that its formation occurs after the late ossification of the lower edge of the posterior atlanto-occipital membrane. Le Double [22] claimed that the DP represents the ligaments' acquired ossification induced by VA pulsation, while Barge [3] supported the theory of special osteogenic potency activation in craniocervical junction area.

A prevalence of 13.6% for the PDP, 9.1% for CDP, 2.7% for PLP, 2.6% for CLP, and 1.2% for CDLP was recorded [28, 29]. Pekala et al. [28, 29] found that Africans had the highest prevalence of PDP (30.2%) followed by North Americans (14.8%), Indians (14.7%), Europeans (12.5%) and South Koreans (11.5%), while Turks had the lowest (9.2%). North Americans had the highest prevalence of CDP (11.3%) followed by Europeans (11.2%), while the lowest prevalence

Table 5 Measurements by age and overall

Total	Age						Overall (244 V)		p*	
	20–39 years (52 V)		40–59 years (70 V)		60 years and above (122 V)					
	Mean ± SD		Mean ± SD		Mean ± SD		Mean ± SD			
Side	Right	Left	Right	Left	Right	Left	Right	Left	Right	Left
TF max diameter	8.02 ± 0.70	7.95 ± 1.12	7.85 ± 0.98	7.61 ± 1.08	7.82 ± 0.98	7.78 ± 1.06	7.86 ± 0.95	7.76 ± 1.07	0.709	0.516
TF min diameter	6.21 ± 0.71	6.30 ± 0.85	6.36 ± 0.70	6.20 0.97	6.09 ± 0.81	6.13 ± 0.97	6.17 ± 0.77	6.17 ± 0.95	0.199	0.779
VAG length	18.84 ± 2.95	19.12 ± 2.52	19.61 ± 2.70	20.72 ± 2.63	18.62 ± 3.15	19.85 ± 2.17	18.90 ± 3.03	19.97 ± 2.38	0.256	**0.043**
PA min height	3.94 ± 1.06	3.79 ± 0.81	3.96 ± 0.93	3.82 ± 0.77	4.25 ± 1.20	3.90 ± 0.94	4.13 ± 1.12	3.86 ± 0.88	0.310	0.846
PA height (outer of VAG)	7.54 ± 1.27	7.37 ± 1.56	8.94 ± 1.50	8.60 ± 1.82	8.23 ± 1.28	8.24 ± 1.25	8.33 ± 1.40	8.22 ± 1.50	**0.001**	**0.014**
D1	12.58 ± 1.41	13.50 ± 1.53	13.72 ± 1.08	13.57 ± 2.03	14.73 ± 1.96	14.48 ± 1.62	13.71 ± 1.76	13.87 ± 1.78	**< 0.001**	**0.034**
D2	15.26 ± 0.93	17.90 ± 2.52	17.06 ± 0.44	18.23 ± 2.01	18.99 ± 2.37	19.19 ± 2.51	17.16 ± 2.15	18.46 ± 2.40	**< 0.001**	0.065
D3	20.44 ± 1.77	20.86 ± 2.16	21.78 ± 1.99	20.94 ± 2.58	21.84 ± 4.04	21.49 ± 1.81	21.37 ± 2.88	21.11 ± 2.20	0.079	0.426
D4	25.29 ± 2.17	26.31 ± 2.93	26.82 ± 1.73	27.18 ± 2.83	26.99 ± 2.08	27.95 ± 2.41	26.39 ± 2.12	27.17 ± 2.78	**0.001**	**0.048**

Bold values indicate the statistical significant impact of the age

*p values from ANOVA

TF transverse foramen, *AF* arcuate foramen, *VAG* vertebral artery groove, *PA* posterior arch, linear distance of VAG from the posterior midline to the most medial edge of VAG on inner (D_1) and outer (D_2) cortices, and to the most lateral edge of VAG to the inner (D_3) and outer (D_4) cortices, *R* right, *L* left side, *V* vertebrae

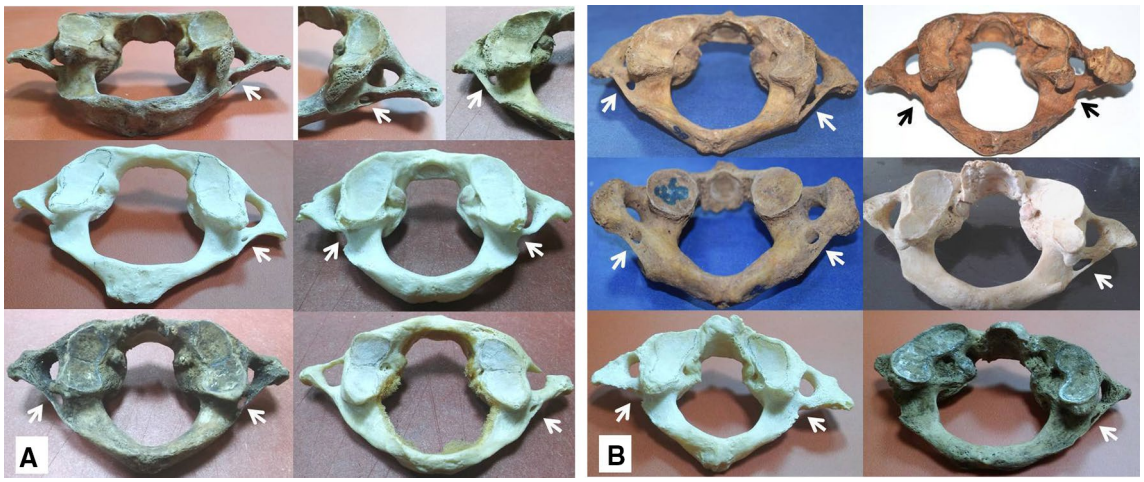

Fig. 3 **a**, **b** Accessory transverse or retrotransverse foramina (depicted with white arrows)

Fig. 4 Open-type transverse foramina unilaterally (depicted with white arrows)

occurred in Asians (7.5%). The CLP was most prevalent in Asia and Africa (2.9%) followed by Europe (2.1%) and the PLP was most prevalent in Africa (11.1%), followed by Asia (1.9%) and Europe (1.0%). The CDLP was most prevalent in Europe (1.4%), followed by Asia (0.8%) [28, 29]. The highest incidences among Europeans appeared for all variants in our study, as DP occurred frequently (54.5%), while LP was less common (5.3%). The PDP was detected in 36.89%, CDP in 22.13%, PLP in 7.78% and CLP in 5.32%. DP and LP coexistence was found in 9.4%. Hassan et al. [16] found low incidences of ossified variants (CDP in 3.42%, PDP in 3.14%, PLP in 2% and CDLP in 1.14%).

Concerning laterality, Dhall et al. [10] and Hasan et al. [16] found left side predominance for the DP. They [10] justified asymmetry from the fact that the majority of people are right-handed, thus the right-sided sternocleidomastoid muscle would be stronger in order to bend the head to the contralateral side. Pekala et al. [28] found laterality for the CDP (46.9% in total, 53.7% on the L and 46.3% on the R). The PDP was detected in 52.3% unilaterally and side symmetry existed (almost equal rates on the R and L, 50.5 and 49.5%) [28]. Current study underlines side symmetry regarding DP and LP existence.

The CDP was more commonly detected in males than females, as gender might influence complete ossification via hormones [35], as in our study (10.4% males vs 7.3% females). Contrariwise, the PDP was more commonly observed in females (18.5%) than in males (16.7%), as well as the CLP. Karau et al. [19] agreed with our results as they found the ponticles more frequently in females and proposed estrogen as a possible factor influencing their ossification.

Sanchis-Gimeno et al. [33] found a high incidence of dehiscent TF (11%) in Caucasians (8% in males, 3% in females), 6% unilaterally and 5% bilaterally, while a total incidence in a mixed population 7.8% (5.5% in males and 2.3% in females), 4.6% unilaterally and 3.2% bilaterally. Seven dehiscent TF were detected (2.9%) on the R and three TF (1.2%) on the L in our sample. In a single vertebra, a dehiscent TF was bilaterally found and in another vertebra, the TF was of contact type on the R. TF were absent in two cases (0.8%) on the R. Dehiscent TF may expose vertebral vessels at injury risk. Moreover, a double TF may be correlated with VA duplication, phenomenon that may mislead surgeons intra-operatively and cause imaging misinterpretation.

The RTF carries a small anastomotic vein connecting suboccipital cavernous sinus with VA venous plexus [4]. Its existence can lead to symptoms such as headache, migraine and fainting attacks [4, 33]. Sanchis-Gimeno et al. [33]

Table 6 Posterior arch (PA) height at vertebral artery groove (VAG) area at the right side (R), left side (L) and in total among studies

Authors	Year	PA height at VAG R (mm)	PA height at VAG L (mm)	PA height at VAG in total (mm)	Observations
Ebraheim et al. [11]	1998			4.1 ± 1.2	
Tan et al. [40]	2003	4.72 ± 0.68	4.58 ± 0.65		8% (4/50) cases < 3.72
Ma et al. [24]	2005			3.88 ± 0.52 inner 1/3 4.25 ± 0.51 outer 1/3	
Sengul and Kodiglu [36]	2006			5.05	
Christensen et al. [6].	2007				7.5% < 3.5
De Carvalho et al. [9]	2009	3.87 ± 0.83	3.92 ± 1.10		
Ravichandran et al. [31]	2011	4.7 ± 0.98	4.55 ± 0.84		
Gosavi and Vatsalaswamy [13]	2012	3.72 ± 1.06	3.70 ± 1.06		65/100 cases < 4
Hassan et al. [16]	2013			3.99	
Ansari et al. [1]	2015	3.79 ± 1.08	4.05 ± 0.086		
Patel and Gupta [27]	2016	4.15 ± 1.28	3.99 ± 1.28		
Rekha and Divya Shanthi [32]	2016	3.68	3.70		
Present study	2018	4.13 ± 1.11	3.86 ± 0.87		

found an incidence of RTF in 9% (5% bilaterally and 4% unilaterally) (6% in males and 3% in females). A similar incidence 7.8% (5% unilaterally and 2.8% bilaterally) (3.7% in males and 4.1% in females) was detected in a mixed population [33]. RTF with lower (1.5%) [8] and higher incidences (25.5%) [19] were observed in Indians. In the present study, closed RTF were detected in 41 cases (16.8%) on the R and in 27 cases (11.1%) on the L, while dehiscent RTF in 22 cases (9%) on the R and in 26 cases (10.7%) on the L.

Posterior arch (PA) and vertebral artery groove (VAG) morphometry

Gosavi and Vatsalaswamy [13] found the mean PA height of the outer part of VAG in 8.61 ± 1.77 mm. In the present study, the mean PA height was 8.32 ± 1.40 mm on the R and 8.21 ± 1.50 mm on the L, and asymmetry existed. Gender dimorphism was observed only on the R (males 8.61 ± 1.44 mm and females 8.02 ± 1.29 mm), although mean values on the L were predominant for males (8.45 ± 1.47 mm) versus females (7.95 ± 1.49 mm).

The mean PA height at the most thin part of VAG (VAG thickness) was found at 5.05 mm by Sengul and Kadioglu [36]. Ma et al. [24] found the mean VAG thickness (4.25 ± 0.51 mm) on the outer 1/3 of PA and mentioned this part as ideal for screw placement to decrease the VA injury risk. Similar values were recorded in the current study with a mean VAG thickness 4.13 ± 1.12 mm on the R and 3.86 ± 0.88 mm on the L (side asymmetry). Various authors discussed about the safe surgical zone on PA to avoid VA injury (Table 6). Tan et al. [40] found in 8% of the reported cases, a PA height to be less than 4 mm (i.e. these dimensions would preclude the PA as the starting point for LM screws), and Gosavi and Vatsalaswamy [13] found the lowest values (3.72 mm on the R and 3.70 mm on the L).

Christensen et al. study [6] underlines the importance of a pre-operative 3D-CT scan of PA at VAG and adequate reconstruction to select cases for safe screw placement, as well as the actual screw's length. Christensen et al. [6] and Huang et al. [17] have placed LM screws through the lower portion of PA in cases with pedicle height of less than 4.0 mm. Screw insertion into the LM through PA is preferable than LM screws since excessive venous bleeding from the large venous plexus surrounding axis and VA, and greater occipital nerve irritation may occur. In addition, if VA courses abnormally below PA, screw insertion at the inferior LM could be risky [6]. Although it is referred that the optimal starting point for a LM screw is at the inferior 1/3 of PA, this area presents significant anatomical variability, and safe LM screw placement is often not feasible. Some surgeons prefer to mobilize VA when placing a screw through a pedicle analog of small bony dimensions. Bodon et al. [4] supported that in case of a DP, the ideal entry point was just below the lateral edge of the inferior bony spicule on PA.

Gupta [15] found the mean VAG length in 11.72 ± 1.8 mm on the R and 12.47 ± 1.9 mm on the L, in Indian skulls. The current study recorded a higher mean length of 18.9 ± 3.03 mm on the R and 19.97 ± 2.38 mm on the L. The distance between C_1 midline and VAG carries surgical importance, as it might be helpful in avoiding or reducing complications, such as VA injury and cranial nerve damage during C_1 stabilization. In the present study, the distance from the midline to the most medial edge of VAG on the inner cortex (D1) was 13.71 ± 1.76 mm (R)

Table 7 Linear distances (in mm) of the vertebral artery groove (VAG) on the superior surface of the atlas from the posterior midline to the most medial edge of the VAG on inner (D_1) and outer (D_2) cortices, and to the most lateral edge of the VAG to the inner (D_3) and outer (D_4) cortices according to various authors

Authors	Year	D_1 R (mm)	D_1 L(mm)	D_2 R(mm)	D_2 L(mm)	D_3 R(mm)	D_3 L(mm)	D_4 R(mm)	D_4 L (mm)
Ebraheim et al. [11]	1998	8.0 10.4 ± 1.70 (M) 8.9 ± 0.80 (F) Safe zone 8–12 (10 for M and 9 for F)		12.00 19.00 (M) and 17.00 (F)					
Senoglu et al. [37]	2006	12.52 ± 2.10 13.65 ± 2.70*		19.55 ± 3.10 22.81 ± 2.20*		12.63 ± 2.10 13.71 ± 2.40*		19.36 ± 2.90 22.64 ± 2.20*	
Sengul & Kodiglu [36]	2006	10.30 ± 1.60	10.40 ± 2.00	16.20 ± 2.50	15.80 ± 2.40				
De Carvalho et al. [9]	2009	10.96 ± 2.03	11.27 ± 2.18	18.83 ± 3.03	18.87 ± 2.43	14.18 ± 2.36	14.26 ± 1.71	23.01 ± 2.79	23.85 ± 2.17
Ravichandran et al. [31]	2011	11.46 ± 1.62	11.06 ± 1.61	17.04 ± 1.97	17.82 ± 1.70	14.26 ± 1.69	14.30 ± 2.03	22.70 ± 1.84	23.14 ± 1.65
Gupta et al. [14]	2013	1.28 cm	1.38 cm					2.30 cm	2.20 cm
El-S Hassanein [12]	2013	11.44 ± 2.91	11.81 ± 3.08	17.08 ± 3.74	18.08 ± 3.74	16.03 ± 3.68	16.56 ± 3.69	18.31 ± 3.70	19.12 ± 3.58
Khanfour et al. [20]	2014	8.60 ± 1.80	8.7 ± 1.5					18.20 ± 2.20	16.50 ± 1.90
Ansari et al. [1]	2015	10.73 ± 2.92 (7.8–20)	9.72 ± 2.56 (6–17.8)					24.85 ± 2.78	24.39 ± 2.06
Patel and Gupta [27]	2016	10.34 ± 1.94	10.3 ± 1.72	14.93 ± 2.30	15.10 ± 2.26				
Present study	2018	13.71 ± 1.77	13.92 ± 1.67	17.15 ± 2.18	18.46 ± 2.39	21.37 ± 2.92	21.10 ± 1.94	26.39 ± 2.17	27.17 ± 2.68

The plethora of published studies calculated the diagonal or vertical distance from the midline of the posterior arch to the proximal and distal inner and outer cortexes of the vertebral artery groove. However, the comparison between mean values is incorrect as according to the Pythagorean Theorem we know that the diagonal distance will always be higher than the vertical

*In ossified variants, *M* males and *F* females

and 13.87 ± 1.78 mm (L), and on the outer cortex (D2) was 17.16 ± 2.15 mm (R) and 18.46 ± 2.40 mm (L). The distance between the midline to the most lateral edge of VAG on the inner cortex (D3) was 21.37 ± 2.88 mm (R) and 21.11 ± 2.20 mm (L), and on the outer cortex (D4) was 26.39 ± 2.12 mm (R) and 27.17 ± 2.78 mm (L). Variable mean values of these distances among ethnic groups are summarized in Table 7. These distances have higher mean values, in cases of ossified variants [45].

Clinical implications

The presence of a CDP and an AF was associated with VA atherosclerosis [26], musculoskeletal pain [7], chronic tension type and cervicogenic headache, migraine, neuralgia and hearing loss [21]. CDP and CLP may cause vertebrobasilar insufficiency, posterior circulation stroke or even death by thrombosis, embolism or arterial dissection [26] due to VA entrapment and repetitive injury of the artery [21].

Detailed knowledge of VAG variants in correlation with PA morphometry is important to avoid intra-operative complications, such as VA injury and neural trauma, especially during lateral dissection and C_1 decompressive laminectomy, LM or pedicle screw insertion [43]. The close proximity of VA to the screw path, the variable location of VA and isthmus narrowing are causative factors for these types of injuries. The existence of C_1 ponticles can also alter surgical planning. During C_1 screw insertion using the classical technique with the entry point between PA and LM, to avoid significant venous bleeding and C_2 nerve root injury, surgeons frequent prefer to place the screw at a higher point, i.e. at the posterior aspect of the PA. However, this placement can result in VA injury, especially if the artery crosses the AF [2]. Additionally, the presence of a CDP may incorrectly provide the impression of a broader PA [7, 43], enforcing surgeon to insert large screws into DP, increasing, therefore, the risk of VA injury [28]. In these occasions, the entry point of screw insertion can be the dorsal aspect of PA instead of the base of the LM or the PA and LM junction. In cases of a wide DP or a deep VAG, it is safer to resect DP prior to screw insertion [45].

DP and LP variants should be carefully identified preoperatively on lateral radiography, before LM screw

placement. Also, screw insertion into the inferior LM can be dangerous in cases of a persistent first intersegmental artery, where the VA courses abnormally below PA. 3D-CT scan may reveal further morphological details of the identified ossified variants, like thinner bridges, although this modality would expose patients to an out of limits radiation [37]. Moreover, CTA can provide valuable information on VA morphology, such as identification of possible side dominance with relevant surgical considerations especially if the dominant artery is located on the side of VAG anomaly [44]. Specifically, a 3D-CTA can depict a much more detailed anatomical delineation for both osseous and vascular structures in the craniocervical junction and, hence, possible injury risks can be recognized in advance [41]. Thus, the surgeon can select the exact entry point and screw trajectory. As there are gender differences in PA and VAG morphometry, surgery in female patients should be approached more cautiously [39]. There is also evidence to support the safety and effectiveness of intra-operative navigation during C_1 screw placement, since its use has been associated with high accuracy and minimal complications [18, 38].

Conclusions

The classification of partial and complete types of DP and LP, and possible combinations is a new approach which allows a punctual interpretation of the ossified structures. Current data may be useful in avoiding VA injury during PA fixation with transarticular or LM or pedicle screws. Unfamiliarity with certain aspects of the surrounding neurovascular structures and lack of experience with the procedure can make C_1 posterior screw placement extremely challenging. Thus, before inserting a screw surgeons are strongly advised to carefully examine cervical spine tomography and angiography, and reconstruction to ensure the type, location, size and shape of C_1 ponticles and VA course. Cases of hypoplastic TF or PA asymmetry should be pre-operatively identified and boundaries must be carefully outlined to achieve a safe exposure of the VA. Technological advances in the field of navigation and intra-operative imaging are expected to enhance surgical safety and accuracy.

Author contributions KN: project development, data analysis, classification system, manuscript editing and final approval, ETP: data collection, data analysis, schematic drawings, PPT, MF and NL: manuscript editing, AS: data analysis, manuscript editing, MK: data analysis, and MP: project development, data collection, data analysis and manuscript editing.

Compliance with ethical standards

Conflict of interest There is no conflict of interest.

Informed consent The authors of the current study express their gratitude to the body donors who donated their bodies before death (written informed consent) and throughout this act; their vertebrae were used for this study.

References

1. Ansari MS, Singla M, Ravi KS, Goel P (2015) Morphometric analysis of atlas and its clinical significance: an anatomical study of indian human atlas vertebrae. Indian J Neurosurg 4:92–97
2. Arslan D, Ozer MA, Govsa F, Kıtıs O (2018) The ponticulus posticus as risk factor for screw insertion into the first cervical lateral mass. World Neurosurg 113:579–585. https://doi.org/10.1016/j.wneu.2018.02.100 **(Epub 2018 Feb 25)**
3. Barge JAJ (1918) Problems in kranio-vertebral Gebiet section. Verh K Akad Wetensch Amsterdam 20(2):102–105
4. Bodon G, Grimm A, Hirt B, Seifarth H (2016) Applied anatomy of screw placement via the posterior arch of the atlas and anatomy-based refinements of the technique. Eur J Orthop Surg Traumatol 26:793–803
5. Chevrel JP, Pineau H, Delmas A (1965) L'arc postérieur de l'atlas, ses variations, étude morphologique et statistique. CR Assoc Anat 50:280–288
6. Christensen DM, Eastlack RK, Lynch JJ, Yaszemski MJ, Currier BL (2007) C1 anatomy and dimensions relative to lateral mass screw placement. Spine 32:844–848
7. Cirpan S, Yonguc GN, Edizer M, Mas NG, Magden AO (2017) Foramen arcuale: a rare morphological variation located in atlas vertebrae. Surgi Radiol Anat 39(8):877–884
8. Srijit Das, Suri R, Kapur V (2005) Double foramen transversarium. An osteological study with clinical implications. Int Med J 12:311–313
9. De Carvalho MF, Rocha RT, Monteiro JTS, Pereira CU, Leite RF, Defino HLA (2009) Vertebral artery groove anatomy. Acta Ortop Bras 17:50–54
10. Dhall U, Chhabra S, Dhall JC (1993) Bilateral asymmetry in bridges and superior articular facets of atlas vertebra. J Anat Soc India 42:23–27
11. Ebraheim NA, Xu R, Lin D, Ahmad M, Heck BE (1998) The quantitative anatomy of the vertebral artery groove of atlas and its relation to the posterior atlanto-axial approach. Spine 23:320–323
12. El-S Hassanein GH (2013) Injury risk of vertebral artery during screw placement through atlas posterior arch. Basic Sci Med 2:21–23
13. Gosavi SN, Vatsalaswamy P (2012) Morphometric study of the atlas vertebra using manual method. Malays Orthop J 6:18–20
14. Gupta C, Radhakrishnan P, Palimar V, D'Souza AS, Kiruba NL (2013) A quantitative analysis of atlas vertebrae and its abnormalities. J Morphol Sci 30(Suppl 2):77–81
15. Gupta T (2008) Quantitative anatomy of vertebral artery groove on the posterior arch of atlas in relation to spinal surgical procedures. Surg Radiol Anat 30:239–242
16. Hasan M, Shukla S, Siddiqui MS, Singh D (2001) Posterolateral tunnels and ponticuli in human atlas vertebrae. J Anat 199:339–343
17. Huang DG, He SM, Pan JW, Hui H, Hu HM, He BR, Li H, Zhang XF, Hao DJ (2014) Is the 4 mm height of the vertebral artery groove really a limitation of C1 pedicle screw insertion? Eur Spine J 23:1109–1114
18. Ishak B, Schneider T, Tubbs RS, Gimmy V, Younsi A, Unterberg AW, Kiening KL (2017) Modified posterior C1 lateral mass screw insertion for type II odontoid process fractures using

intraoperative computed tomography-based spinal navigation to minimize postoperative occipital neuralgia. World Neurosurg 107:194–201
19. Karau PB, Ogeng'o JA, Hassanali J, Odula P (2010) Anatomy and prevalence of atlas vertebrae bridges in a Kenyan population: an osteological study. Clin Anat 23:649–653
20. Khanfour AA, El Sekily NM (2015) Relation of the vertebral artery segment from C1 to C2 vertebrae: an anatomical study. Alexandria J Med 51:143–151
21. Koutsouraki E, Avdelidi E, Michmizos D, Kapsali SE, Costa V, Baloyannis S (2010) Kimmerle's anomaly as a possible causative factor of chronic tension-type headaches and neurosensory hearing loss: case report and literature review. Int J Neurosci 120:236–239
22. Le Double AF (1912) Traité des variations de la colonne vertébrale de l'homme. Vigot, Paris
23. Le Minor JM (1997) The retrotransverse foramen of the human atlas vertebra: a distinctive variant within primates. Acta Anat (Basel) 160(3):208–212
24. Ma X-Y, Yin Q-S, Wu Z-H, Xia H, Lu J-F, Zhong S-Z (2005) Anatomic considerations for the pedicle screw placement in the first cervical vertebra. Spine 30:1519–1523
25. Macalister A (1869) Notes on the homologies and comparative anatomy of the atlas and axis. J Anat 3:54–64
26. Ouyang ZY, Qiu MJ, Zhao Z, Wu XB, Tong LS (2017) Congenital anomaly of the posterior arch of the atlas: a rare risk factor for posterior circulation stroke. J Neurointerventional Surg 9(7):e27
27. Patel NP, Gupta DS (2016) A morphometric study of adult human atlas vertebrae in South Gujarat population, India. Int J Res Med Sci 4:4380–4386
28. Pękala PA, Henry BM, Pękala JR, Hsieh WC, Vikse J, Sanna B, Walocha JA, Tubbs RS, Tomaszewski KA (2017) Prevalence of foramen arcuale and its clinical significance: a meta-analysis of 55,985 subjects. J Neurosurg Spine 27:276–290
29. Pękala PA, Henry BM, Phan K, Pękala JR, Taterra D, Walocha JA, Tubbs RS, Tomaszewski KA (2018) Presence of a foramen arcuale as a possible cause for headaches and migraine: systematic review and meta-analysis. J Clin Neurosci 54:113–118
30. Radojevic S, Negovanovic B (1963) La gouttière et les anneaux osseux de l'artère vertébrale de l'atlas. Acta Anat (Basel) 55:186–194
31. Ravichandan ND, Shanthi KC, Shrinivasan V (2011) Vertebral artery groove in the atlas and its clinical significance. J Clin Diagnos Res 5:542–545
32. Rekha BS, D'Sa Divya Shanthi (2016) Morphometric anatomy of the atlas (C1) vertebra among Karnataka population in India. Int J Anat Res 4:1981–1984
33. Sanchis-Gimeno JA, Llido S, Perez-Bermejo M, Nalla S (2018) Prevalence of anatomic variations of the atlas vertebra. Spine J. 2018
34. Sato E, Noriyasu S (1978) Studies on the ponticulus posterior and ponticulus lateralis of the human first cervical vertebra. Sapporo Med J 47:599–617
35. Saunders SR, Popovich S (1978) A family study of two skeletal variants: atlas bridging and clinoid bridging. Am J Phys Anthropol 49:193–204
36. Sengul G, Kadioglu HH (2006) Morphometric anatomy of atlas and axis vertebra. Turkish Neurosurgery 16:69–76
37. Senoglu M, Gümüşalan Y, Yüksel KZ, Uzel M, Celik M, Ozbag D (2006) The effect of posterior bridging of C-1 on craniovertebral junction surgery. J Neurosurg Spine 5:50–52
38. Smith JD, Jack MM, Harn NR, Bertsch JR, Arnold PM (2016) Screw placement accuracy and outcomes following O-Arm-navigated atlantoaxial fusion: a feasibility study. Global Spine J 6:344–349
39. Song MS, Lee HJ, Kim JT, Kim JH, Hong JT (2017) Ponticulus posticus: morphometric analysis and Its anatomical Implications for occipito-cervical fusion. Clin Neurol Neurosurg 157:76–81
40. Tan M, Wang H, Wang W, Zhang G, Yi P, Li Z, Wei H, Yang F (2003) Morphometric evaluation of screw fixation in atlas via posterior arch and lateral mass. Spine 28:888–895
41. Vaněk P, Bradáč O, de Lacy P, Konopková R, Lacman J, Beneš V (2017) Vertebral artery and osseous anomalies characteristic at the craniocervical junction diagnosed by CT and 3D CT angiography in normal Czech population: analysis of 511 consecutive patients. Neurosurg Rev 40:369–376
42. Von Torklus D, Gele W (1972) The upper cervical spine. Grune and Stratton, New York, pp 28–30
43. Wright NM, Lauryssen C (1998) Vertebral artery injury in C1–C2 transarticular screw fixation: results of a surgery of the AANS/CNS section on disorders of the spine and peripheral nerves. J Neurosurg 88:634–640
44. Yamaguchi S, Eguchi K, Kiura Y, Takeda M, Kurisu K (2008) Posterolateral protrusion of the vertebral artery over the posterior arch of the atlas: quantitative anatomical study using three-dimensional computed tomography angiography. J Neurosurg Spine 9:167–174
45. Yeom JS, Kafle D, Nguyen NQ, Noh W, Park KW, Chang BS, Lee CK, Riew KD (2012) Routine insertion of the lateral mass screw via the posterior arch for C1 fixation: feasibility and related complications. Spine J 12:476–483